Received: 6 October 2022 | Accepted: 22 November 2022

DOI: 10.1002/pamm.202200111

3D FEM Simulation of Titanium Alloy (Ti6Al4V) Machining with Harmonic Endmill Tools

Abraham Kalu-Uka[1,2,*], **Chigbogu Ozoegwu**[2,**], and **Peter Eberhard**[1,***]

[1] Institute of Engineering and Computational Mechanics, University of Stuttgart, Germany
[2] Department of Mechanical Engineering, University of Nigeria, Nsukka, Nigeria

Usually, end milling operations have been carried out using conventional uniform helix tools with fixed helix angles. Thus, many studies have been conducted to study the effects of these tools on the thermomechanical properties of a milling process. Recently, there have been works that point to the benefits of using harmonic endmills. Harmonic endmills consist of cutting edge profiles that have continuously harmonically varying helix angles. The variation is described using a harmonic function of axial position (elevation) of points on the cutting edge. In this work, a 3D finite element simulation using ABAQUS, is carried out for the complex milling process of Titanium alloy Ti6Al4V. The envelope of the harmonic tool is first generated using a set of MATLAB codes and stored in a Standard Triangle Language (.stl) format. The machine tool is introduced into an FEM program which has been designed to provide for dynamic effects, thermo-mechanical coupling, material damage law and the criterion for contact associated with the milling process. A Johnson-Cook material constitutive equation which combines the effects of strain hardening, strain softening, and temperature softening is used. To account for the chip separation criterion, the Johnson Cook damage evolution equation is used. The milling process simulation for Ti6Al4V is then carried out. In the end, the stress distribution and the cutting forces are obtained.

1 Introduction

In milling processes, there have always been efforts to find ways of reducing cutting forces to save energy costs. Furthermore, the ability to accurately predict cutting forces and other thermo-mechanical milling properties, has great research and industrial benefits, especially in avoiding wasting money, time, and other resources in physical experiments [1]. To this effect, FEM simulation tools, which can predict and visualize the milling process, have become very useful. With the development of materials with highly improved mechanical properties, the need came up to design endmill tool geometries which can handle complex materials while reducing cutting forces.

Titanium alloy (Ti6Al4V) has an excellent combination of high specific strength, fracture resistance, high resistance to corrosion and oxidation, and biocompatibility [2, 3]. These characteristics yield wide application in the aerospace industry, deep-sea operations, and medical equipment production [4]. On the other hand, it has poor machinability and is extremely difficult to cut because of its low thermal conductivity and high chemical reactivity with materials of the cutting tool. For these reasons, numerous research works have been carried out to improve the milling of Ti6Al4V. There have been many studies like [5, 6] which considered the effects of cutting conditions like cutting speed, feed speed, etc. in milling the alloy. Other studies considered the effects of arbitrary tool geometric parameters like constant helix angle, constant pitch angle, number of flutes and rake angle on the milling process [7, 8]. The effects of tool edge radius increment (which arise because of tool wear) on heat generation, tool wear rate and chip flow were studied by [9]. The generation of heat fluxes in the components that interact during milling process (milling tool, workpiece and chips); and the temperature distribution within them, were studied by [10, 17, 18]. In addition, works like [1, 2, 11] studied the effects of various deformation behaviour of Ti6Al4V alloy, (based on their material constitutive deformation properties), on stresses and cutting forces. However, there have been very little studies on the effect of the variable helix angle of an endmill tool on a milling process, with [13] comparing the experimental and numerical performance of cutting force on wave form tools. Then, [14] analyzed the cutting forces acting on end milling tools which have variable free-form helix angle profiles. This existing knowledge gap gives rise to the need to carry out a study on the effects that a variable helix-shaped endmill tool geometry would have on milling Ti6Al4V.

2 Research Methodology

2.1 Modeling Strategy

A typical endmill tool shown in Fig. 1, see [15], has shape geometric parameters that include rake angle, helix angle, clearance angle, relief angle, and pitch angle. For this study, the helix angle, also called cutting edge inclination angle, is chosen as the control parameter. The choice of this parameter is based on its significant influence in defining the helix shape of the cutting

* Corresponding author: e-mail abraham.kalu-uka@itm.uni-stuttgart.de, phone +49 711 685 64724, fax +49 711 685 6400
** Email chigbogu.ozoegwu@unn.edu.ng
*** Email peter.eberhard@itm.uni-stuttgart.de

edge of a tool, [8, 12], as it helps to smoothen and extend the duration and geometric length of contact between a cutting edge and a workpiece, hence reducing impacts if appropriately selected [14]. Two endmill tools with different helix-shape profiles will be considered here: a standard tool and a harmonic tool, as shown in Figs. 2(a) and 2(b). Both tools have two flutes with a constant pitch angle of 180^0 and rake angle of 0^0. They also have the same diameter of 20 mm. However, they have different helix-shaped profiles. The standard tool has a constant helix angle of 25^0 while the harmonic tool has a range of variable helix angles, having a mean value of 25^0.
Equation 1, see [14], that describes the harmonic tool is

$$\beta_z = C\left(1 + \lambda \sin\left(\frac{2\pi n}{z} w_h + \phi\right)\right) = C + \alpha_h \sin\left(\frac{2\pi}{L_h \cos C} z + \phi\right) \quad , \tag{1}$$

where n is 10 and is the number of wave cycles needed in the depth range of the helix profile, w_h, is 30 mm. The value of ϕ is 0^0 and is the phase angle of the variation, a_h, equal to $C\lambda$ is the amplitude of the variation with C having a value of 25^0 as the mean helix angle. The control parameter for the amplitude, λ = 0.5, is used to define the amplitude of harmonic variation about the flute mean helix angle C, assuming that n is an integer. It falls in the range $-1 \leq |\lambda|$. There is a special case for $\lambda = 0$, in which the harmonic profile becomes a standard profile. The wavelength is $L_h = w_h / n \cos C$.

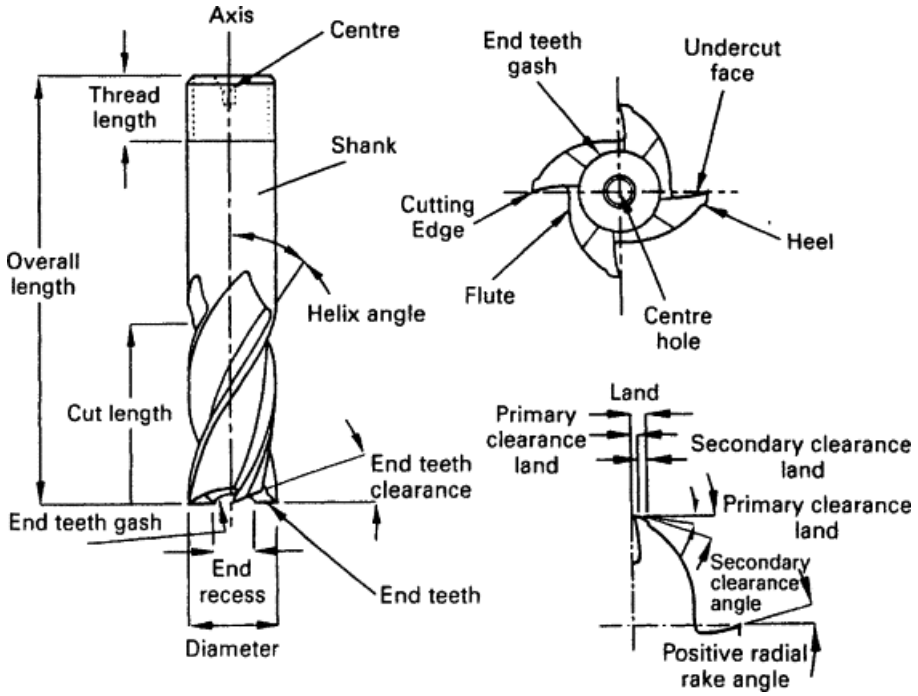

Fig. 1: A typical endmill tool geometry, taken from [15].

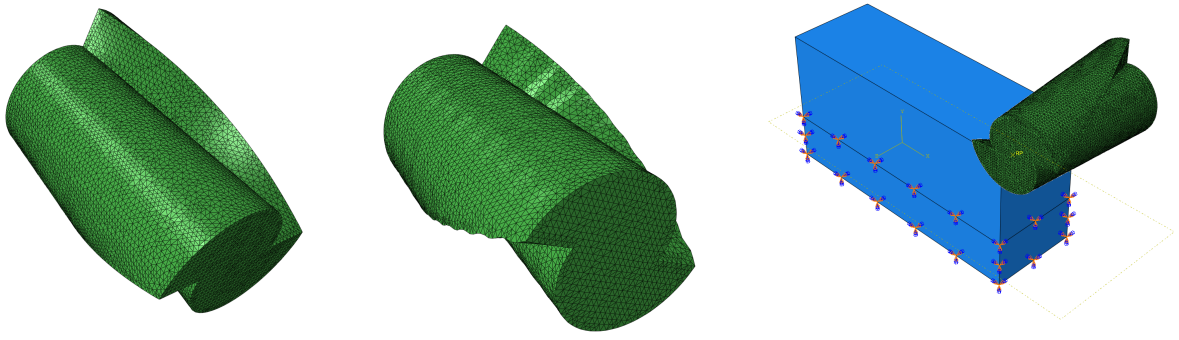

(a) standard tool (b) harmonic tool (c) tool-workpiece assembly

Fig. 2: An illustration of the two endmill tools and a tool-workpiece assembly showing the boundary conditions.

2.2 Simulation Model

The ABAQUS finite element software is used to simulate the milling process of a Ti6Al4V workpiece, using two different endmill tools (standard and harmonic tool). First, the geometries of the cutting tool and workpiece are developed and meshed, and the material properties are defined. The governing and constitutive equations are applied. The selection of the required field outputs in an endmilling operation is made after setting the simulation step and boundary conditions. Then the contact relationship between tool and workpiece is established. Finally, simulations are run and results of stress and force distribution are analyzed.

The dimensions of the workpiece are 60 mm×20 mm×30 mm. The numerical model for the workpiece is made up of 384,000 hex elements, and the element type is C3D8R. The harmonic tool is set as rigid and has 13466 triangular surface elements while the standard tool, also set as rigid, has 16954 triangular surface elements (both are of R3D3 element type). The axial depth of cut is 20 mm while the radial depth of cut is set to 4 mm. The time integration method used is Dynamic Explicit for determining stress distribution and forces. The bottom of the workpiece is firmly fixed in position using the Encastre boundary condition while the tool can rotate and also move against the workpiece, Fig. 2(c). The spindle speed is 105 rad/s while the effective feed rate is 0.09 m/s.

2.3 Material Constitutive Equation, Damage Criterion and Friction Model

2.3.1 Johnson-Cook Material Model

To analyze a milling process using numerical FE methods, the information of the material constitutive behaviour under severe loading conditions is required [8]. The Johnson-Cook, (JC), material law, which is applicable to dynamic problems involving large deformations and high strain rate temperature effects, is used in this simulation for Ti6Al4V. This material law gives the expression for the flow stress that occur during plastic deformation and has been widely applied in numerical studies for deformation processes [1]. It describes the stress-strain response along with the strain hardening effects, strain rate hardening, and thermal softening. The flow stress is expressed as

$$\sigma = (A + B\epsilon^n)\left[1 + C\left(\ln\frac{\hat{\epsilon}}{\hat{\epsilon_0}}\right)\right]\left[1 - \left(\frac{T - T_0}{T_m - T_0}\right)^m\right] \quad , \tag{2}$$

where *A, B, C, m, n* represent the initial yield stress, hardening modulus, strain rate sensitivity coefficient, work hardening exponent, and thermal softening coefficient respectively. The equivalent stress is σ, $\hat{\epsilon}$ is the plastic strain rate, $\hat{\epsilon_0}$ is the reference strain rate, T_0 is the reference temperature, T_m is the melting temperature, and T is the temperature of the material cutting zone.

2.3.2 Johnson–Cook Damage Evolution Criterion

To account for fracture or damage in the material, the JC damage evolution criterion is used. This criterion gives the expression for the equivalent plastic strain which describes the influence of strain, strain rate, and temperature, in bringing about material fracture. When the equivalent plastic strain attains a certain criteria value required for material separation from the workpiece, damage initiation takes place, which leads to chip formation.The JC damage evolution criterion is

$$\epsilon_f = \left(D_1 + D_2\exp\left(-D_3\frac{p}{q}\right)\right)\left[1 + D_4\ln\frac{\hat{\epsilon}}{\hat{\epsilon_0}}\right]\left[1 + D_5\left(\frac{T - T_0}{T_m - T_0}\right)\right] \quad , \tag{3}$$

where D_1, D_2, D_3, D_4, and D_5 are initial failure strain, exponent factor, triaxiality factor, strain rate factor, and temperature factor, respectively, and p is the hydrostatic pressure and q is the von Mises stress.

2.3.3 Coulomb's Friction Model

The Coulomb friction model is used to describe the contact interaction between the tool and developing chips. To apply this model, it is assumed that the frictional stress on the cutter is proportional to the normal stress with a constant friction coefficient. Two regions can be observed during contact: sliding region and sticking region, see [7]. The sliding region shows linear relation between frictional and normal stress, while in the sticking region, the shear stress is constant and equal to the critical stress. These regions are expressed as:

1. for sticking region,

$$\tau_f = k_c, \quad \text{for} \quad \mu\sigma_n \geq k_c \tag{4}$$

2. for sliding region,

$$\tau_f = \mu\sigma_n, \quad \text{for} \quad \mu\sigma_n < k_c \quad , \tag{5}$$

where σ_n is the normal stress, τ_f is the frictional tangential stress, k_c is the shear flow stress of the material, and μ is the friction coefficient which is assumed to be 0.1 in the simulation.

Table 1: Physical properties of Ti6Al4V alloy

density (kg/m^3)	elastic modulus (GPA)	Poisson ratio	thermal conductivity (W/mK)	linear expansivity ($10^{-6}/°C$)	specific heat capacity (kJ/kg)
4430	110	0.33	6.6	7.5	670

Table 2: Parameters of Johnson-Cook constitutive equation for Ti6Al4V alloy, taken from [16].

A (MPa)	B (MPa)	C	n	m	$\hat{\epsilon}_0$
1098	1092	0.014	0.93	1.1	1

Table 3: Parameters of Johnson-Cook damage (fracture) for Ti6Al4V alloy, taken from [16].

D_1	D_2	D_3	D_4	D_5	$\hat{\epsilon}_0$
-0.09	0.25	-0.5	0.014	3.87	1

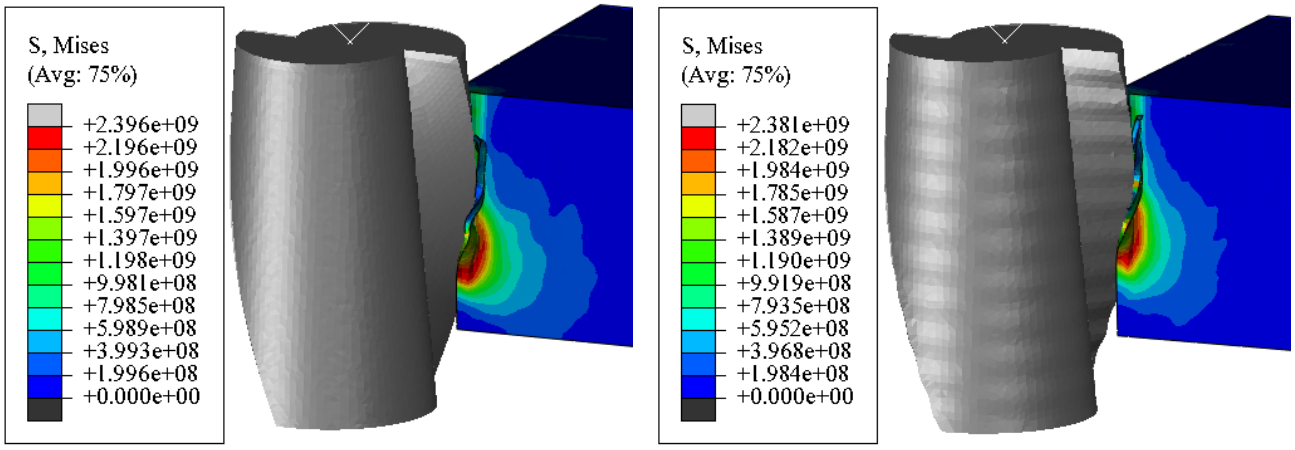

(a) milling with standard tool (b) milling with harmonic tool

Fig. 3: Stress distribution of Ti6Al4V milling process at midpoint of the workpiece

3 Results and Discussion

Stress is induced as the endmill tool engages the workpiece material and damage develops gradually as the helical cutting edge goes forward in each revolution of the tool. When the damage variables reach their limit, the elements fail and get removed from the model. In Figs. 3(a) and (b), the cutting position is at the midway point along the axial depth of the workpiece, for each tool. This occurs at a time 0.023 s for the standard tool and 0.022 s for the harmonic tool, when the elements have been partially separated from the workpiece (chip formation). For a total cutting time of 0.2 s, the maximum von Mises stress recorded for the standard and harmonic tools are 2.396 *G*Pa and 2.381 *G*Pa, respectively. To determine the various peak force values, the average value of the ten highest force values is calculated. Whereas the feed forces and the feed normal forces are negative values, the axial forces are positive values. The feed and feed normal force values are negative because the tool cuts through the workpiece along the negative x and z directions. The axial force values are positive because the simulation process is up milling and cutting force is directed upward in the positive y direction in an up milling process. For the peak feed force, Fig. 4(a), the harmonic tool exerts only 69.55 *k*N compared to 81.35 *k*N for the standard tool. The peak axial forces, Fig. 4(b), are 37.33 *k*N and 49.2 *k*N for the harmonic and the standard tool, respectively. The peak feed normal forces, Fig. 4(c), are 27.4 *k*N and 33.04 *k*N for the harmonic and the standard tool, respectively. The peak resultant forces, Fig. 4(d) are 83.35 *k*N for the harmonic tool and 99.91 *k*N for the standard tool. The highest force reduction occurs in the determination of the peak axial force value, which is the force component required to totally separate the developing chip from the workpiece. Considering all force components, the harmonic tool recorded lower stresses and cutting forces compared to the standard tool. It is important to point out that the magnitude of these forces are higher than those obtained in similar studies [7,8] that are related to cutting forces. This is because the values which are used in this study for the axial depth of cut, 20 mm, and the radial depth of cut, 4mm, are high when compared to the values used in those studies. Investigation is ongoing to understand the reason for the reductions in the force values (for the harmonic tool) in order to accurately explain the parametric characteristics responsible for them and then to maximize this benefit through the optimization of the harmonic shape parameters.

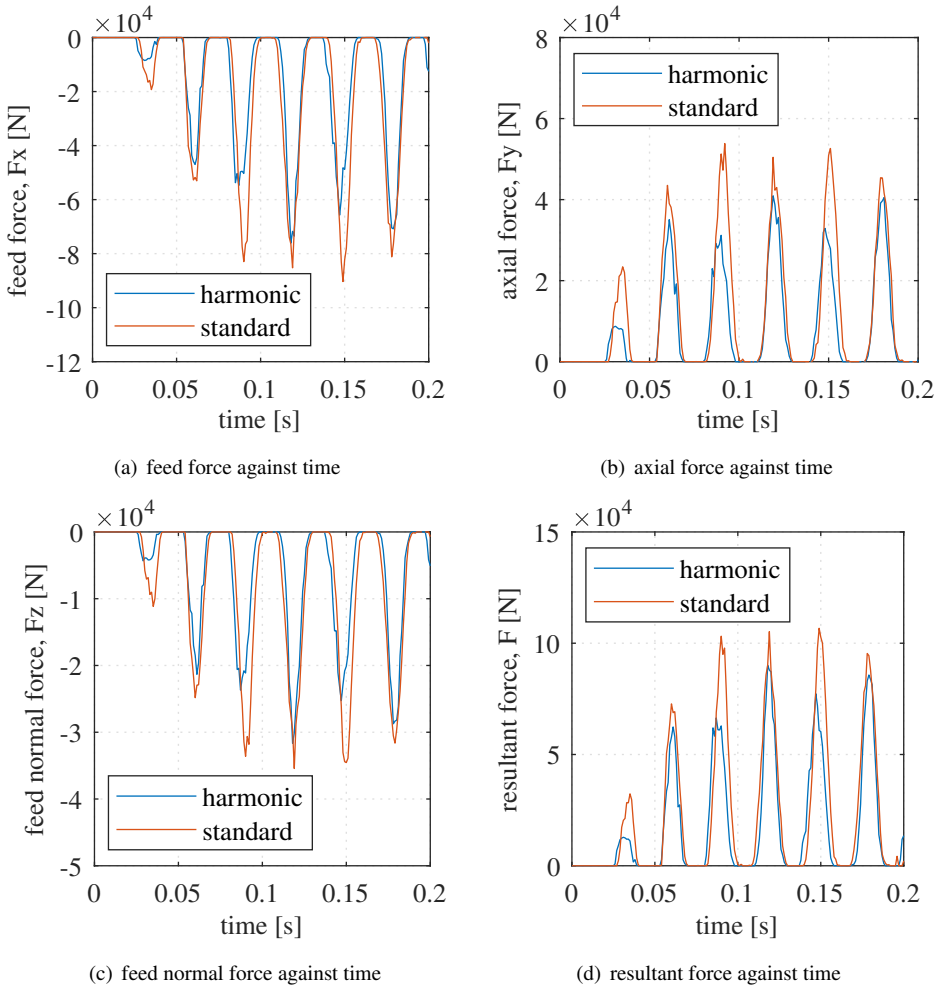

(a) feed force against time

(b) axial force against time

(c) feed normal force against time

(d) resultant force against time

Fig. 4: Cutting forces over time.

4 Conclusion

The commercial Abaqus/Explicit FEM tool has been used to simulate the milling process of Ti6Al4V using two different tool geometries (standard and harmonic). The maximum stress induced while using the standard tool for a total cutting time of 0.2s is 2.396 *G*Pa and is higher than that induced while using the harmonic tool which is 2.381 *G*Pa. The percentage decrease in the peak forces of the feed, axial, feed normal, and resultant motions of the harmonic tool relative to the standard tool are 14.51%, 24.12%, 17.04% and 17.58%, respectively. Thus, the harmonic tool with variable helix angle shows some improvement in stress and force reduction during a Ti6Al4V milling process.

Acknowledgements The first author is thankful to the Deutscher Akademischer Austauschdienst (DAAD) for funding this research. The second author is currently doing research at the University of Stuttgart funded by the Alexander-von-Humboldt Foundation (AvH). All support is gratefully acknowledged. Open access funding enabled and organized by Projekt DEAL.

References

[1] K. S. Sekar, and M. Kumar, Finite element simulations of Ti6Al4V titanium alloy machining to assess material model parameters of the Johnson-Cook constitutive equation, *Journal of the Brazillian Society of Mechanical Sciences and Engineering* volume 33:2, pages 203-211 (2011).

[2] M. Yaich, Y. Ayed, Z. Bouaziz, and G. Germain, Numerical analysis of constitutive coefficients effects on FE simulation of the 2D orthogonal cutting process: application to the Ti6Al4V, *International Journal of Advanced Manufacturing Technology* volume 93, pages 283-303 (2017).

[3] T. Ozel, and M. Sima, Finite element simulation of high speed machining Ti6Al4V alloy using modified material models, *Transactions of NAMRI/SME* volume 38, pages 49-56 (2010).

[4] Z. Ren, X. Zhang, Y. Wang, Z. Li and Z. Liu, Finite element analysis of the milling of Ti6Al4V titanium alloy laser additive manufacturing parts, *Applied Sciences* volume 11, pages 4813-4826 (2021).

[5] C. Ji, Y. Li, X. Qin, Q. Zhao, D. Sun, and Y. Jin, 3D FEM simulation of helical milling hole process for titanium alloy Ti6Al4V, *International Journal of Advanced Manufacturing Technology* volume 81, pages 1733-1742 (2015).
[6] M. Vrabel, N. Durakbasa, P. Kovac and I. Mankova, Contribution to the FEM simulation of Ti6Al4V machining, *Acta Mechanica Slovaca* volume 21:1, pages 54-61 (2017).
[7] H. B. Wu, and S. Zhang, 3D FEM simulation of milling process for titanium alloy Ti6Al4V, *International Journal of Advanced Manufacturing Technology* volume 71, pages 1319-1326 (2014).
[8] A. Li, J. Zhao, Z. Pei, and N. Zhu, Simulation-based solid carbide end mill design and geometry optimization, *International Journal of Advanced Manufacturing Technology* volume 71, pages 1889-1900 (2014).
[9] T. Thepsonthi, and T. Ozel, 3-D finite element process simulation of micro-end milling of Ti6Al4V titanium alloy: Experimental validations on chip flow and tool wear, *Journal of Materials Processing Technology* volume 221, pages 128-145 (2015).
[10] B. Kumar, K. Reddy, and R. Kumar, Finite element model based on Abaqus/Explicit to analyze the temperature effects of turning, *International Journal of Applied Engineering Research* volume 11, pages 5728-5734 (2016).
[11] J. Lu, J. Chen, Q. Fang, B. Liu, Y. Liu, and T, Jin, Finite element simulation for Ti6Al4V alloy deformation near the exit of orthogonal cutting, *International Journal of Advanced Manufacturing Technology* volume 85, pages 2377-2388 (2016).
[12] M. Wan, J. Feng, W. Zhang, Y. Yang, and Y. Ma, Working mechanism of helix angle on peak cutting forces together with its design theory for peripheral milling tools, *Journal of Materials Processing Technology* volume 249, pages 570-580 (2017).
[13] K. Aydin, A. Akgun, C. Yavas, A. Gok, and U. Seker, Experimental and numerical study of cutting force performance of wave form end mills on gray cast iron, *Arabian Journal for Science and Engineering* volume 46, pages 12299-12307 (2021).
[14] C. Ozoegwu, and P. Eberhard, Geometric definition, rapid prototyping, and cutting force analysis of cylindrical milling tools with arbitrary helix angle variations, *Journal of Engineering Manufacture* volume 236:9, pages 1232-1246 (2022).
[15] S. Black, A. Lissaman, V. Chiles, and S. Martin, *Principles of Engineering Manufacture*, Butterworth-Heinemann, Elsevier Science, 1996, pp. 316-370.
[16] Y. Zhang, J. Outeiro, and T. Mabrouki, On the selection of Johnson-Cook constitutive model parameters for Ti6Al4V using three types of numerical models of orthogonal cutting, *Proceedings: 15th CIRP Conference on Modelling of Machining Operations*, Karlsruhe, Germany, CIRP 31 Elsevier, Karlsruhe, 2015, pp. 112-117.
[17] M. Putz, G. Schmidt, U. Semmler, M. Dix, M. Braunig, M. Brockmann, and S. Gierlings, Heat flux in cutting: importance, simulation, and validation, *Proceedings: 15th CIRP Conference on Modelling of Machining Operations*, Karlsruhe, Germany, CIRP 31 Elsevier, Karlsruhe, 2015, pp. 334-339.
[18] M. Putz, C. Oppermann, M. Braunig, and U. Karaguzel, Heat sources and fluxes in milling: comparison of numerical, analytical and experimental results, *Proceedings: 16th CIRP Conference on Modelling of Machining Operations*, Cluny, France, CIRP 58 Elsevier, Cluny, 2017, pp. 97-103.

